Optical Communication and Navigation for Spacecraft Docking using Modulating Retroreflectors

Linda M. Wasiczko[+], Harris R. Burris[§], N. Glenn Creamer[+], Rita Mahon[*], Christopher Moore[+], Lee Swingen[+], James Murphy[+], Mena Stell[§], Brad E. Pinney[+], Peter Goetz[+], William J. Scharpf[+], William S. Rabinovich[+], and G. Charmaine Gilbreath[+]

[+] U.S. Naval Research Laboratory, 4555 Overlook Ave., SW, Washington, DC 20375

[§] Research Support Instruments, 4325-B Forbes Blvd, Lanham, MD 20706

*Titan/Jaycor, 1410 Spring Hill Rd., McLean, VA 22102

ABSTRACT

An optical communications link is used to transmit important navigation and range information between two spacecraft platforms to aid in the spacecraft docking process. This experiment uses NRL's multiple quantum well modulating retroreflector (MRR) array as the light payload optical communications transmitter on the target spacecraft. Spacecraft navigation information is determined by using the MRR array to impose five distinct modulation frequencies on the optical transmit beam, and analyzing the received signal on the pursuer spacecraft to extract target attitude and range information. Design, architecture, and status of the experiment at NRL are discussed.

1. Introduction

In the past few years, many enabling technologies have been developed to support autonomous spacecraft docking[1]. These technologies include global positioning system (GPS) sensing, video guidance sensors[2], lidar[3], and radio frequency (RF) communication links. These systems normally require an active payload on the target, add significant power and/or mass to the spacecraft, or have a limited field of view. Another limitation is the range of the rendezvous system. Previously proposed rendezvous and docking systems are built upon limited range subsystems that must handoff to one another during the rendezvous and docking process[3,4]. A more attractive solution would be a single rendezvous and docking system to support short range rendezvous (1-3 km), proximity operations (<1 km), and final docking (<10 m).

In this paper, a novel system for spacecraft rendezvous, docking, and navigation using a multiple quantum well (MQW) modulating retroreflector (MRR) array is presented. The MRR array may be used over ranges up to 3 km or more, may use eyesafe interrogators at 1550nm, provide ranging data with centimeter accuracy, and establish an interference-free communication channel between the target and pursuer spacecraft. The only active source in this system would be on the interrogator side; therefore, the payload on the pursuer spacecraft would be a very low power payload. A potential enhancement to the system would be to add a second, optimized optical train into the interrogator to enhance precision during close-in operations.

2. Multiple Quantum Well Modulating Retroreflectors

A modulating retroreflector is hybrid solution built upon basic optics and solid state technology. A simple solid corner cube retroreflector redirects incident energy along the same propagation path as the interrogating beam. The corner cube retroreflector's directionality and wide field-of-view make the element an interesting choice for a passive communication device. The multiple quantum well (MQW) modulator transforms the capability of the retroreflector. The MQW modulator behaves like a shutter, and changes the transmission of light that has been reflected through the retroreflector. The combined modulating retroreflector device is essentially a lightweight, low power, shutter that provides the on-off

Free-Space Laser Communications V, edited by David G. Voelz, Jennifer C. Ricklin, Proc. of SPIE Vol. 5892
(SPIE, Bellingham, WA, 2005) · 0277-786X/05/$15 · doi: 10.1117/12.621747

Report Documentation Page

Form Approved
OMB No. 0704-0188

1. REPORT DATE **2005**	2. REPORT TYPE	3. DATES COVERED **00-00-2005 to 00-00-2005**

4. TITLE AND SUBTITLE **Optical Communication and Navigation for Spacecraft Docking using Modulating Retroreflectors**	5a. CONTRACT NUMBER 5b. GRANT NUMBER 5c. PROGRAM ELEMENT NUMBER
6. AUTHOR(S)	5d. PROJECT NUMBER 5e. TASK NUMBER 5f. WORK UNIT NUMBER
7. PERFORMING ORGANIZATION NAME(S) AND ADDRESS(ES) **Naval Research Laboratory,4555 Overlook Avenue, SW,Washington,DC,20375**	8. PERFORMING ORGANIZATION REPORT NUMBER
9. SPONSORING/MONITORING AGENCY NAME(S) AND ADDRESS(ES)	10. SPONSOR/MONITOR'S ACRONYM(S) 11. SPONSOR/MONITOR'S REPORT NUMBER(S)

12. DISTRIBUTION/AVAILABILITY STATEMENT
Approved for public release; distribution unlimited

13. SUPPLEMENTARY NOTES
The original document contains color images.

14. ABSTRACT

15. SUBJECT TERMS

16. SECURITY CLASSIFICATION OF:			17. LIMITATION OF ABSTRACT	18. NUMBER OF PAGES	19a. NAME OF RESPONSIBLE PERSON
a. REPORT **unclassified**	b. ABSTRACT **unclassified**	c. THIS PAGE **unclassified**		**9**	

Standard Form 298 (Rev. 8-98)
Prescribed by ANSI Std Z39-18

keying capability required for a line-of-sight optical communications link. These devices also have the advantage of being radiation hard.

The modulators used in this experiment are designed for operation near 1550nm. The MQW modulators are epitaxial structures of InGaAs/InAlAs grown on InP substrates. Further details on the growth of the MQW modulators can be found in Ref. 5. An applied voltage changes the absorption of the MQW modulator, which is the shuttering mechanism used to generate the high and low optical data bits under illumination. The operating principle of the MQW modulating retroreflector is shown in Fig. 1. A measurement of the optical absorption of an InGaAs/InAlAs MQW modulator across a range of wavelengths is shown in Fig. 2. Typical contrast ratios for MRRs at 1550nm are between 2:1 and 3:1.

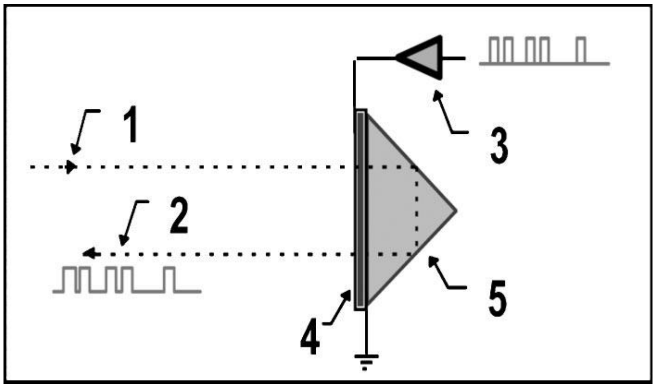

Fig. 1: Operation of the MQW modulating retroreflector: 1. Incident light beam; 2. Outgoing modulated beam after two reflections; 3. Applied external bias; 4. MQW modulator; 5. Solid corner cube retroreflector. (Figure from Ref. 5).

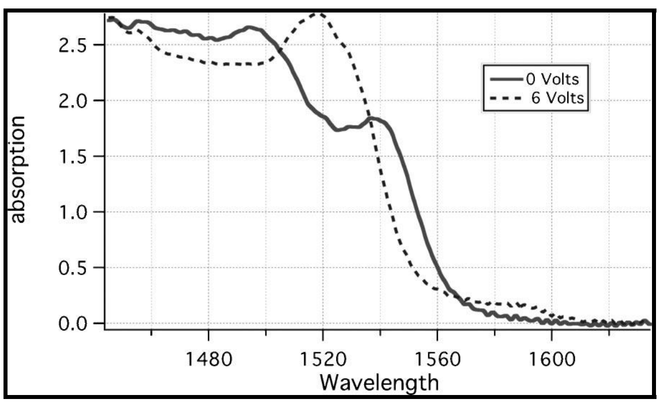

Fig. 2: Optical absorption versus wavelength of the InGaAs/InAlAs MQW modulator. Bias voltages of 0 Volts and 6 Volts were applied. (Figure from Ref. 5).

The maximum data rate of a MQW MRR device is a function of its RC time constant. The RC time constant is dependent on device size and electrode configuration. The MQW MRRs used in this experiment have 0.63 cm diameters, allowing for data rates up to 10 Mbps. Therefore, the MRR platform could provide a high speed communications channel between the target and pursuer spacecraft. There is a limit to the length of the communications channel proportional to the inverse of the range to the fourth power. The received optical power scaling law for a diffraction-limited system is[1]:

$$P_{received} \propto \frac{P_{laser} D_{retro}^4 D_{rec}^2}{\theta_{div}^2 L^2 \lambda^2}$$

Where P_{laser} is the optical power of the laser transmitter, D_{retro} is the diameter of the retroreflector, D_{rec} is the diameter of the receiver aperture, θ_{div} is the laser transmitter divergence, L is the range between the transmitter and MRR platforms, and λ is the laser wavelength.

3. Interspacecraft Rendezvous and Docking Methodology

Strengthening of an automatic rendezvous and docking capability is necessary for NASA's future missions[6]. A drawing of a situation using a MRR array for navigation and docking is shown in Fig. 3. The Target spacecraft possesses only an attitude stabilization capability. It has a MRR array mounted on the side of the spacecraft to be used for communication or docking. The MRR payload places a minimal power draw on the satellite. The Pursuer spacecraft actively navigates to the target, using its attitude and translational control capability. The pursuer spacecraft contains the active laser interrogator and the optical receivers with related timing electronics.

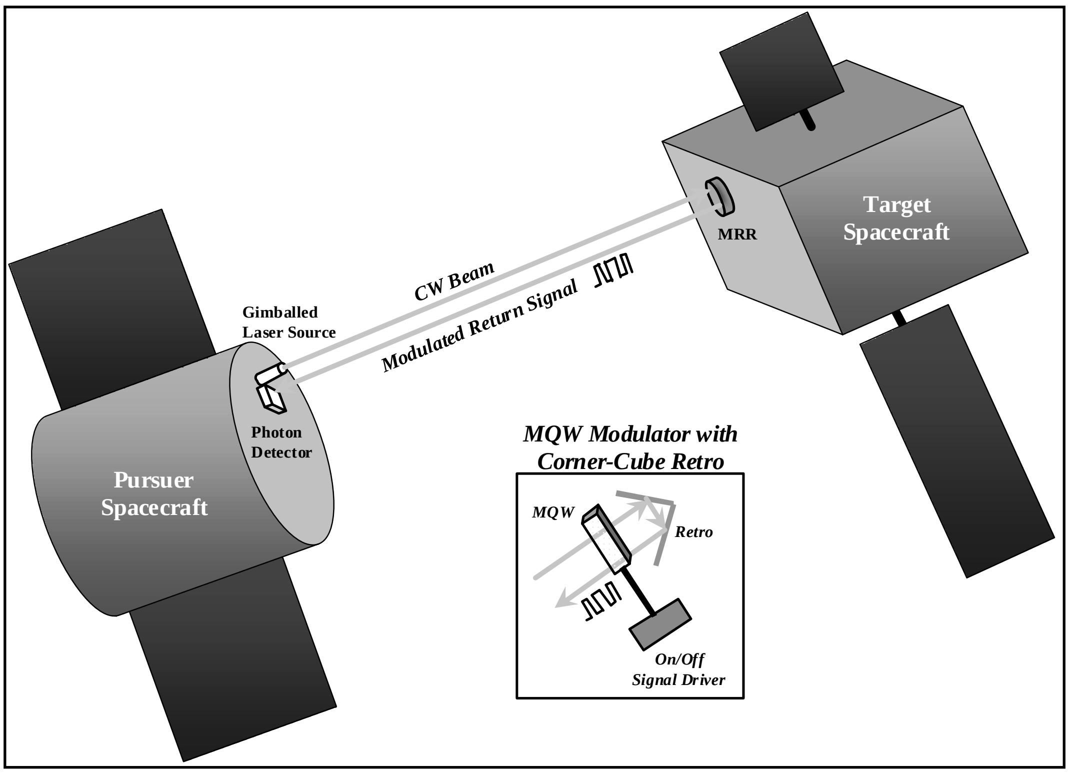

Fig. 3: Navigation and Docking situation between two spacecraft. The active source is located on the Pursuer spacecraft.

The MRR array on the target spacecraft is modulated by a free-running square wave with a 5 Volt amplitude. Each MRR has its own tone, which for this experiment are approximately 1780 Hz, 1865 Hz, 1970 Hz, 2065 Hz, and 2170 Hz. These frequencies were chosen to be within the frequency response of a 13 mm Ge position sensing detector (PSD). In a deployed system, the MRRs would not be modulated freely, but could be kept in a sleep-mode until a beacon on the pursuer activated the array.

The laser interrogator on the pursuer spacecraft has interrogation, ranging, and communication capabilities. For this experiment, only the interrogation and ranging capabilities are used. A drawing of the interrogator is shown in Fig. 4. The interrogator outputs a continuous wave laser beam at 1550 nm. The output laser light is launched downrange after passing through a 50/50 beamsplitter. The beamsplitter picks off a portion of the interrogation signal, which is used to start the timing system for the TOF ranging. After subsequent modulation by the MRR and traversing the 50/50 beam splitter a second time, the modulated light passes through the receiver leg where it is split off to a position sensitive detector and TOF stop pulse detector. The 13 mm Ge position sensing detector (PSD) receives the modulated light, which is digitized by a National Instruments DAQPad 6070E 12-bit A/D board. Near real-time processing in LabVIEW using the appropriate PSD equations gives the (x,y) coordinates and signal strength of each imaged MRR spot on the PSD.

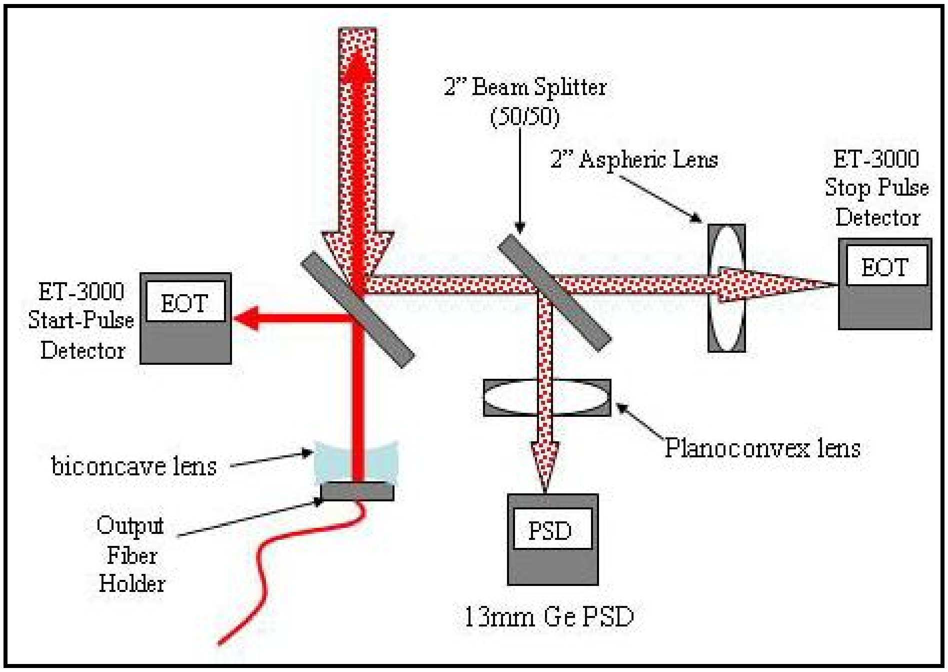

Fig. 4. Laser interrogator on pursuer spacecraft. PSD is used for navigation, while the start- and stop-pulse detectors are used for ranging. Another detector leg could be added in for communications.

The start and stop-pulse detectors are used for ranging at 10Hz. A Stanford Research SR-620 counter measures the time-of-flight range in seconds. The start pulse is generated by dropping the input voltage to the Keopsys optical amplifier every 100 msec using an Analogics polynomial waveform synthesizer Model 2045. The Analogics unit generates a pulse with a fast risetime that only the start and stop pulse detectors can see. The frequency response of the PSD is slow enough that it never sees the fast risetime pulse. Also, since the MRR passes photons even during a '0' bit, ranging can occur accurately at anytime in the pulse train. A drawing of the modulation and ranging scheme is shown in Fig. 5.

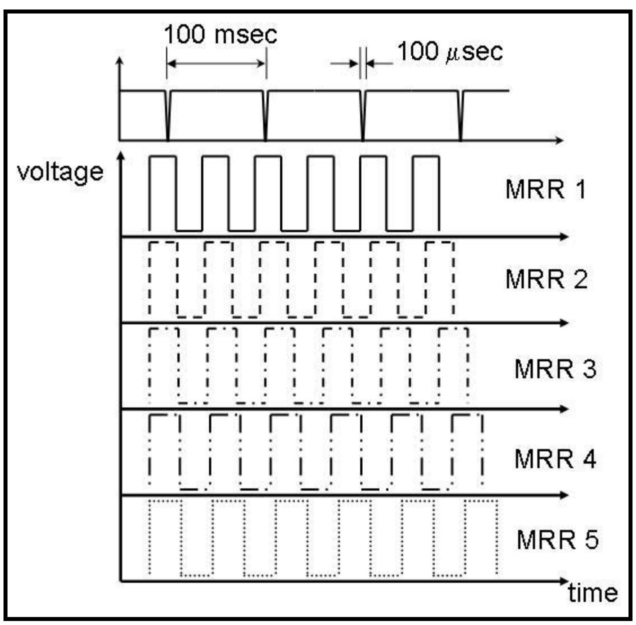

Fig. 5: Modulation of the MRR array and spacing of the time-of-flight laser ranging pulses.

4. Interspacecraft Navigation Equations

Navigation occurs when the optical beam from the laser interrogator is incident on at least one of the MRRs in the array. To aid in coarse tracking and acquisition, the laser interrogator is mounted on a Sagebrush gimbal. The acquisition search pattern was discussed in Ref. 1.

The relative navigation solution is calculated using the perspective projection equations for a camera[7]. In close proximity, these equations can be used to calculate full 6-state pose. Pose is the position and orientation of a specific platform. At longer ranges, at least partial pose may be determined using perspective projection. This data will complement the information given by the time-of-flight ranging system.

5. Initial Experimental Characterization of Navigation and Ranging System

The navigation and ranging software was written in LabVIEW. Acquisition is triggered from the Analogics polynomial waveform synthesizer. Approximately 49 msec of MRR data may be acquired before the ranging pulse interferes with the data signal. Data is digitized to 4096 levels, analyzed in frequency space, and passed to either a file or used as feedback to the gimbal. A sufficient number of samples are read so that the jitter in the Fourier transform algorithm is minimized, which is close to the 49 msec of data before the generation of the ranging pulse. The PSD supports 1μm accuracy for an incident power of 0.1mW. Although we may transmit over 1 Watt of power using the Keopsys EDFA, the losses in the optical train of the interrogator due to the 50/50 beam splitters are significant. The optical system would have to be optimized if the interrogator were to be used in a real scenario.

By analyzing each of the 4 PSD channels at the 5 MRR tones, (x,y) position and spot intensity information are extracted. A plot of the 5 MRR spots extracted from the PSD data is shown in Fig. 6.

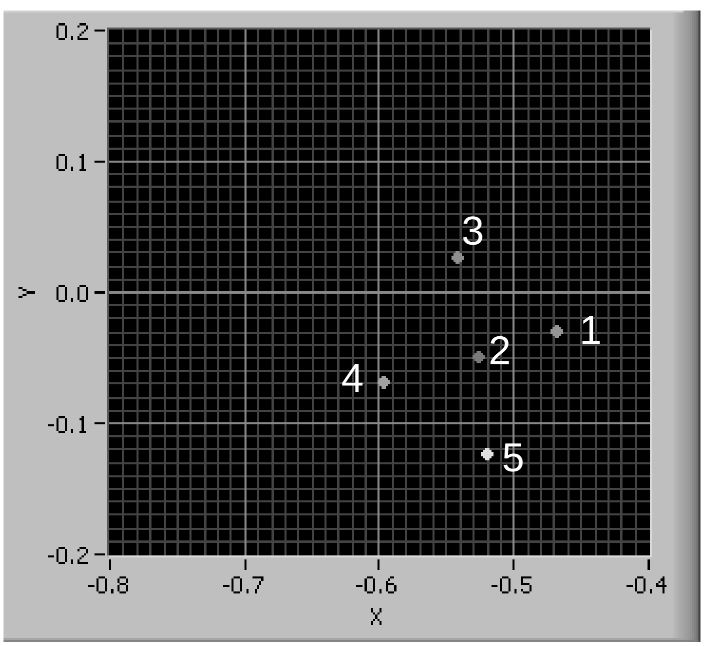

Fig. 6: Image of 5 MRR spots created from PSD data. MRRs are labeled 1 through 5. Each 0.1 separation in (x,y) corresponds to a 650 μm distance on the PSD.

A power spectrum showing the frequency components acquired from the PSD is shown in Fig. 7. Peaks are spaced approximately 100 Hz apart. The central MRR has the tallest peak in the power spectrum, which is expected because the MRR array is illuminated with a Gaussian beam.

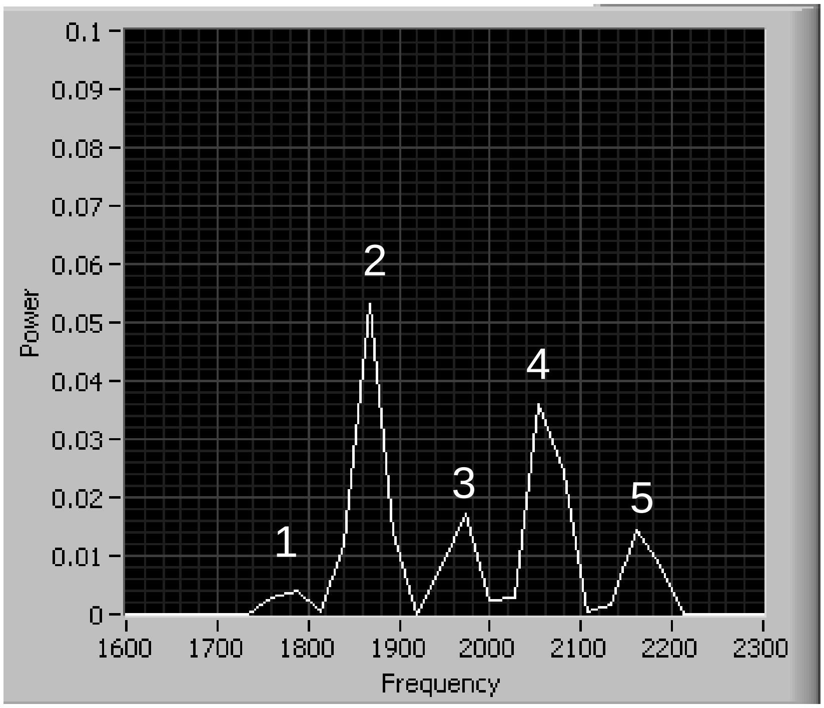

Fig. 7: Power spectrum versus Frequency (Hz) of the received signal on the PSD. The y-axis has units of V_{rms}^2. The labels correspond to the MRR labels in Fig. 6.

Axial perspective changes were demonstrated by turning the array about its vertical axis. The array was roughly aligned perpendicular to the direction of propagation, and the array projection was measured in Fig. 8a. After a rotation of the array through a 13 degree angle from the propagation direction, the array was measured again in Fig. 8b. The width between MRRs 1 and 4 has decreased by 40.5 μm. Recall that the distance between the large grid markers is 650 μm. Noise levels on the PSD are less than 1 μm.

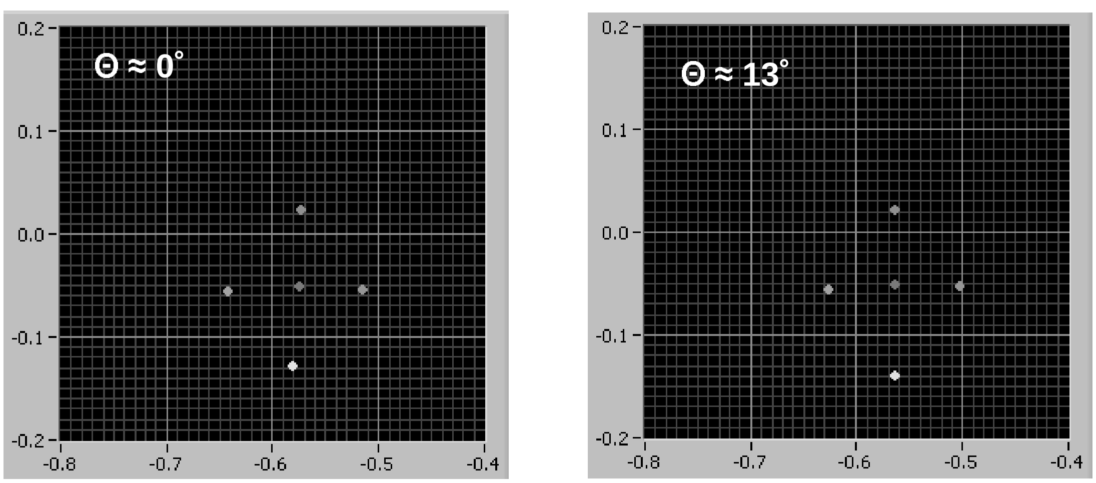

Fig. 8. (a) (left) MRR array on PSD, with MRR area approximately perpendicular to the propagation direction. (b) (right) MRR array on PSD, with MRR turned approximately 13 degrees around its vertical axis.

6. Time-of-Flight Ranging Characterization

Time-of-flight ranging is a well known method of measuring the distance to a target[8]. By precisely measuring the round trip time of a coherent light pulse, the distance to a target can be determined. Time-of-

flight measurements are common to satellite laser ranging[8] and lidar systems[9]. The ranging subsystem within the pursuer laser interrogator was tested in static and moving conditions in the laboratory. The initial interrogator design differs slightly from the one shown in Fig. 4; the biconcave and planoconvex lenses were not necessary at the time since the ranging system was tested with only 1 MRR under illumination. The time-of-flight range is calculated by:

$$Range = \tfrac{1}{2}\left(TOF \times c\right)$$

where c is the speed of light in m/s and TOF is the time-of-flight measured in seconds. The factor of ½ comes from the fact that this is a round-trip measurement.

Accuracy of the ranging subsystem was assessed by setting up a static ranging test. A Tektronix oscilloscope was setup to measure the temporal delay between the outgoing and incoming laser ranging pulses. The data was taken at the full bandwidth of the oscilloscope (500 MHz), which resulted in a timing jitter of 0.2 ns. Results are shown in Fig. 9. As is seen from the figure, most of the data is included within +/- 5 mm of the mean. The standard deviation of the data is 2.89 mm. The data was also measured using only one MRR, instead of the array, to ensure the best measurement accuracy.

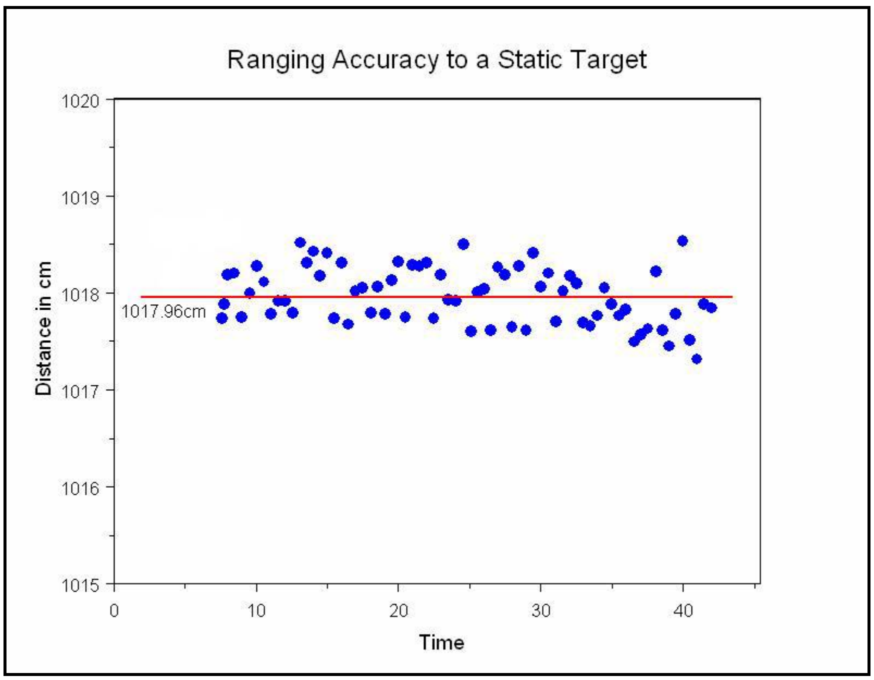

Fig. 9: Range accuracy to a static target. Mean range was calculated to be 1017.96 cm with a standard deviation of 2.89 mm.

A second test measured the relative motion of the MRR in a quasi-sinusoidal pattern along the axis of ranging. The results are shown in Fig. 10. From the data, the target was determined to have moved with a relative range motion of 5.076 cm/s. In spacecraft rendezvous and docking situations, range rate accuracies are required to be on the order of centimeters/second[6].

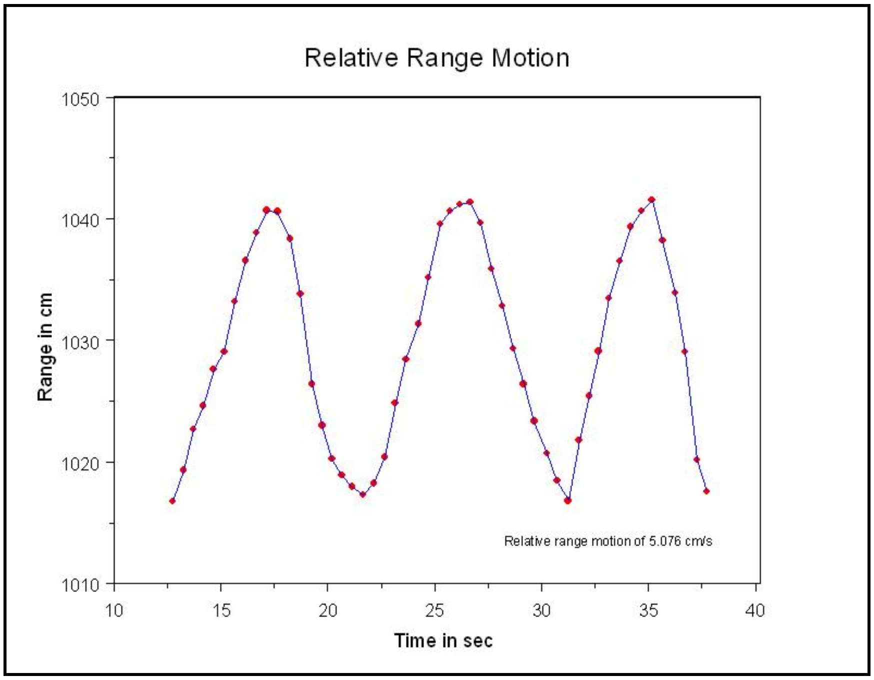

Fig. 10: Ranging to a moving target. The target MRR moved with a relative range motion of 5.076 cm/s.

7. Simultaneous Data Transfer and Ranging

Simultaneous data transfer and time-of-flight ranging was demonstrated in the laboratory. The Analogics PWS Model 2045 generated a ranging pulse every 10 Hz. The video data transfer and ranging operate asynchronously. Glitches in the modulation of the MRR were small enough that video was transferred without interruption at 3 Mbps using an L-3 compression unit. A frame from one video is shown in Fig. 11. The lower trace on the oscilloscope also shows the ranging pulse. Any blurring in the image is an artifact of the video compression by the L-3.

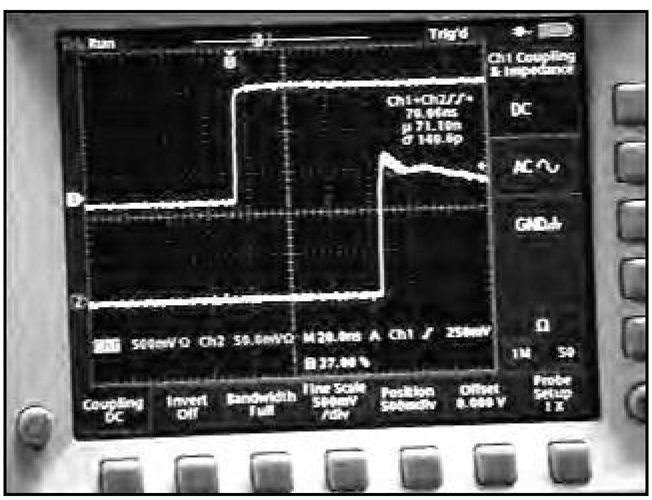

Fig. 11: One frame of live video that was transferred over the MRR laser communication link while simultaneously ranging to the MRR target. Video was transferred at 3 Mbps.

8. Conclusions

A novel interrogator for spacecraft navigation and ranging has been designed and tested in a laboratory environment. The interrogator demonstrated ranging accuracy on the order of a few mm. The navigation system using prospective projection is still being finalized, but initial results looking at the projection of the MRR array on the PSD are encouraging. The interrogator was adapted for simultaneous ranging and video transfer using the modulating retroreflector laser communication link. This is the first report of simultaneous ranging and data transfer over an optical link.

9. References

1. N. Glenn Creamer, et al, “Interspacecraft Optical Communication and Navigation using Modulating Retroreflectors,” Journal of Guidance, Control, And Dynamics, 27(1), p. 100-106, Jan-Feb 2004.
2. F.D. Roe, R.T. Howard, L. Murphy, “Automated rendezvous and capture system development and simulation for NASA,” Proceedings of the SPIE, Modeling, Simulation and Calibration of Space-Based Systems, Vol. 5420, p. 118-125, April 2004.
3. E. Martin, D. Maharaj, et al., “RELAVIS: the development of a 4D laser vision system for spacecraft rendezvous and docking operations,” Proceedings of the SPIE, Spaceborne Sensors, vol. 5418, p. 69-80, April 2004.
4. J.L.Junkins and Hughes, D., "Vision-Based Navigation for Rendezvous, Docking & Proximity Operations," AAS Guidance and Controls Conference, Breckenridge, CO, February 3-7, 1999.
5. W.S. Rabinovich, et al., “Free-space optical communication link at 1550 nm using multiple-quantum-well modulating retroreflectors in a marine environment,” Optical Engineering, vol. 44, no. 5, p. XXX, May 2005.
6. M.E. Polites, “An Assessment of Technology of Automatic Rendezvous and Capture in Space,” NASA Technical Publication, No. 208528, July 1998.
7. E.R. Davies, Machine Vision: Theory, Algorithms, and Practicalities, Morgan Kauffman Publishing, 2004.
8. John J. Degnan, “Millimeter Accuracy Satellite Laser Ranging: A Review,” In: Smith, D.E., Turcotte, D.L. (Eds.), Contributions of Space Geodynamics: Technology. AGU Geodynamics Series, Vol. 25, p. 133-162, 1993.
9. R. Myllylä et al., “Imaging distance measurements using TOF lidar,” J. Optics, Vol. 29, p. 188-193, 1998.